KFUPM
Journal of Undergraduate Research International

Diamond Open Access

Article
Aerospace Engineering

Sensitivity Analysis of CubeSat Orbital Parameters for Enhancing Revisit Time and Regional Coverage: A Case Study of the Najran–Yemen Desert Border

Ghadi Mahdi Al Amer and Asia Saeed Kajo Habila*

Cite https://doi.org/10.64589/juri/222234

Submitted: November 29, 2025 **Revised:** April 03, 2026 **Accepted:** April 09, 2026

ABSTRACT

Frequent satellite observations play an important role in enhancing the security of border regions. However, maintaining adequate coverage by using a single CubeSat remains challenging. This study investigates the feasibility of employing a single CubeSat to monitor the Najran–Yemen desert border by optimizing orbital parameters to minimize revisit time while preserving effective regional coverage. This study aimed to determine the orbital configuration, specifically the optimal values of inclination and right ascension of the ascending node (RAAN) to maximize temporal access to the targeted area. A one-year simulation was conducted using Systems Tool Kit (STK) software, in which a nadir-pointing CMOS sensor with fixed imaging parameters was attached to the CubeSat. Two main orbital scenarios were analyzed: a Sun-synchronous orbit (SSO) and a user-defined orbit with varying inclinations and RAAN values. Coverage and Figure-of-Merit (FoM) tools in STK were used to generate coverage metrics, including the overall coverage percentage. The results reveal that the SSO configuration exhibits very long revisit intervals and limited temporal visibility across the border. In contrast, the optimized orbit reduces the average revisit time by more than one order of magnitude and increases access opportunities by over threefold compared to the SSO baseline, with optimal performance achieved at an inclination of 20° and RAAN = 120°. These findings confirm that careful orbital tuning improves temporal monitoring capability, providing a practical approach for efficient single-satellite border surveillance.

Keywords: CubeSat, earth observation, satellite coverage analysis, revisit time, figure of merit, STK simulation

1. INTRODUCTION

Satellite technology has become a critical component in various fields, including communications, environmental monitoring, and border surveillance[1]. Traditional satellites, however, often entail high costs and face challenges during launch, which limit their deployment. However, recent years have seen a remarkable increase in the utilization and exploration of cube satellites (CubeSats)[2,3], a popular type of nanosatellite. Each CubeSat comprises one or more units, with each unit measuring 10 ×10 ×10 cm and possessing a mass of approximately 1 kg[4]. Owing to their comparatively low manufacturing, launch, and maintenance costs, they have emerged as a promising platform for various applications, including Earth observation and remote sensing[5]. This shift toward miniaturized satellite platforms has motivated researchers to investigate their feasibility for security-sensitive applications.

Using CubeSats to monitor sensitive and dynamic regions such as the desert borders between Saudi Arabia and Yemen presents significant challenges in terms of image quality and revisit time (Figure 1). This region is a critical conduit for the illicit trafficking of weaponry, narcotics, and qat into Saudi Arabia[6]. However, due to the small CubeSat form factor, it is challenging to equip them with cameras capable of achieving both high spatial resolution and wide-swath coverage simultaneously. Moreover, the use of a single CubeSat may also affect access and revisit times. This inherent tradeoff between revisit time and maintaining good imaging quality limits the effectiveness of CubeSats for border monitoring, making it crucial to investigate and evaluate the sensitivity of orbital parameters to balance both objectives.

Research by Selva and Krejci[7] explored various applications of satellite technology in communication systems, disaster monitoring, border surveillance, and military intelligence. Satellites provide reliable, near-real-time, high-resolution data that support both civilian and defense-related activities. For example, communication satellites can transmit information rapidly and securely worldwide. Similarly, large remote-sensing satellites, such as ASTER and Sentinel-2, have been successful in environmental change detection and disaster response. These studies highlight the strategic importance of space-based assets in surveillance operations; however, they primarily focus on large, high-performance satellite platforms.

The high camera specifications, large apertures, and high altitudes of Sentinel 2 and other large satellites provide excellent coverage for various remote-sensing applications. In contrast, CubeSats, with lower-specification imagery systems, orbit at lower altitudes, achieving lower spatial resolution and smaller coverage. These limitations motivated the present study, in which the role of satellites in enhancing regional security and resilience was investigated.

Although a single CubeSat has a significant advantage owing to its reduced system complexity and cost, its ability to provide frequent observations is limited due to longer revisit times. One of the possible ways to overcome such limitations, already pursued in previous works, is the deployment of a multisatellite CubeSat architecture optimized to minimize revisit time. Santilli et al.[8] investigated the potential of CubeSat constellations for disaster management by designing an optimal architecture aimed at minimizing revisit time over remote regions of Brazil. It was demonstrated that deploying multiple CubeSats across appropriately selected orbital planes can reduce revisit intervals. However, constellation-based approaches increase mission complexity, cost, and operational requirements. Furthermore, existing CubeSat coverage studies have largely focused on either constellation design or general Earth observation missions, rather than examining how a single CubeSat can be geometrically optimized for a specific regional security application.

Despite the growing interest in CubeSat-based Earth observation, existing research has not adequately examined how a single CubeSat can be optimally configured for effective border surveillance in desert environments, nor has it addressed context-specific applications within the Kingdom of Saudi Arabia.

To address these challenges, the effective implementation of CubeSats was investigated for continuous security monitoring of the Najran–Yemen desert border by determining the optimal orbital parameters that maximize the revisit frequency over the target area and relying on orbital parameter optimization rather than additional spacecraft. Unlike previous studies that prioritized increasing satellite numbers or enhancing payload capabilities, orbital inclination and right ascension of the ascending node (RAAN) were isolated as controllable design variables in this study; their direct impact on revisit performance was evaluated for a defined border region. The ultimate contribution of this study lies in providing an optimized framework for single-satellite mission design and offering practical insights for enhancing border surveillance using CubeSat systems.

2. METHODS

2.1. CubeSat Platform and Orbital Parameters. A CubeSat with six units, equipped with a fixed solar panel within its body and keeping the nadir face free of panels for camera mounting, was considered in this study. The CubeSat was modeled at an orbital altitude of 500 km above Earth's surface. The key orbital parameters considered as primary variables in the analysis are listed in Table 1. Each parameter was selected based on a typical configuration utilized for Earth observation in low-Earth orbit. A schematic illustration of the fundamental orbital elements is presented in Figure 2 to clarify their geometric meanings within the orbital plane. The two main planes that define most of the parameters are Earth's equatorial plane and the orbital plane defined by the inclination and RAAN.

The inclination range was based on the latitude of the region of interest (ROI), which is near 18° N. Because a satellite can access latitudes only up to its orbital inclination, moderate inclinations slightly higher than the target latitude were expected to concentrate ground track intersections over the region while avoiding unnecessary coverage at higher latitudes. Consequently, low-to-moderate inclinations were evaluated to assess their impact on revisit performance for localized monitoring.

Similarly, RAAN was varied across a broad interval to assess the effect of the orbital plane orientation on the longitudinal ground track alignment. Because RAAN determines the spatial relationship between the orbital plane and Earth's rotation, sweeping this parameter enables the identification of configurations that produce more favorable temporal clustering of accesses over the target area. This approach represents a structured geometric sensitivity analysis based on orbital mechanics principles.

2.2. Sensor and Imaging Model. The simulated CubeSat was assumed to carry a CMOS-based optical sensor, consistent with the CubeSat's constraints, such as low power consumption and high-resolution images during rapid orbital motion[10]. The imaging system pixel resolution was 4096 ×3072 with a 5-µm

Figure 1. Map of the desert border region between Najran, Saudi Arabia, and Yemen[6]

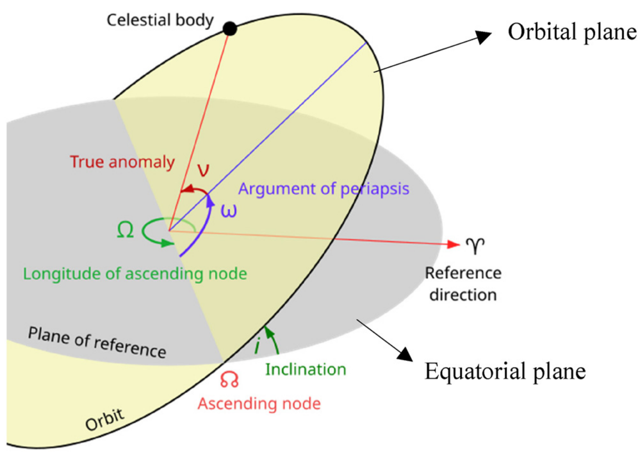

Figure 2. Schematic diagram of orbital elements (adapted from Wikipedia, 2025)

Table 1. *Description of Key Orbital Parameters Used in the Study*

Parameter	Symbol / Unit	Typical Range Tested	Purpose / Effect in simulation
Altitude	h (km)	500	Controls the satellite's height above Earth; affects image resolution, coverage area, and revisit time. Lower altitude means higher resolution but smaller coverage area.
Inclination	i (°)	20–98	Determines the latitude range the satellite can cover. Higher inclinations allow more frequent passes over mid-latitude regions such as the border region targeted in this study.
Right ascension of ascending node (RAAN)	Ω (°)	30–180	Defines the orbit's orientation relative to the Sun and epoch; affects the local time of day when the satellite passes over the target area
Eccentricity	e	0 (circular orbit)	Fixed in this simulation, to simplify the analysis; ensures uniform altitude throughout each orbit.
Argument of perigee	ω (°)	0 (fixed)	Not significant for circular orbits; kept constant in all simulations.

Table 2. *Summary of Scenario 1 (FoM Results)*

Number of Access	Access Duration (s)	Average revisit Time (days)	Average Coverage Percentage (%)
127	9.346	251.73	0.0750

pixel size and a 100-mm focal length, resulting in a rectangular field of view defined by half-angles of 5° (cross-track) and 4° (along-track), corresponding to full angular extents of 10°×8°. The sensor was mounted in a nadir-pointing configuration to maximize scene stability and simplify the geometric projection of the footprint onto the Earth's surface. At an altitude of 500 km, this configuration yields an approximate ground swath of 87.5 km (cross-track) and 70.0 km (along-track), computed using W = 2h/tan(Θ). The GSD, which represents the ground resolution of the image, was estimated by

$$GSD = \frac{H \times P}{f}$$

where H is the satellite altitude, P is the pixel size, and f is the focal length.

Lower GSD values indicate finer image details, whereas higher orbital altitudes result in coarser resolutions. However, both scenarios (described in the next section) simulated in this study were implemented at the same altitude using an identical camera and nadir-pointing configuration; therefore, the GSD values remained constant at approximately 25 m/pixel (at 500 km altitude).

2.3. Overview of STK Simulation and Coverage Analysis. The simulation was conducted using Systems Tool Kit (STK) version 12.9, which is typically used in the aerospace field for spacecraft mission design, analysis, and visualization [11]. Specifically, it is used for modeling, analyzing, and visualizing different space missions, including orbit propagation, sensor geometry, and coverage assessment [12]. In the context of this research, STK was used to model the CubeSat orbit, onboard sensor, and interaction between the satellite and the defined region of interest (ROI) over the simulation period.

In this paper, coverage refers to the number of grid points within the ROI that were observed at least once during the simulation. It is also described using different parameters, such as

- Access duration: Time period during which the grid point is visible to the sensor during a single pass.
- Number of accesses: Total number of distinct access intervals between the sensor and target/grid points.
- Revisit time: Time interval between consecutive access events to the same grid point.
- Coverage percentage: Percentage of grid points that achieved at least one access point during the simulation.

These metrics were obtained using the STK Coverage and Figure of Merit (FoM) tools, which are commonly applied in satellite coverage and revisit analysis studies [13].

Table 3. *Summary of Scenario 2 FoM results*

Inclination	Number of access	Access duration (s)	Average revisit time (days)	Average coverage percentage (%)
20°	335	6.020	9.355	0.1632
25°	267	10.374	12.383	0.2603
30°	203	5.206	8.489	0.0694
40°	168	4.805	11.17	0.0483
98°	122	4.967	18.8	0.0290

Note: The "Number of access" represents the total number of access events recorded by the STK Coverage Definition over the entire ROI during the simulation period. This value corresponds to the cumulative access count across all grid points. In contrast, the "Average revisit time" represents the mean revisit interval computed per grid point using the STK Revisit Time FoM and then averaged over all grid points within the ROI. Because these metrics were computed at different aggregation levels, their numerical values were not directly reciprocal.

2.3.1. Simulation scenario setup and region of interest. The simulation epoch was set to November 17, 2025, 09:00:00 UTCG, and the analysis duration was one year. The initial orbital state was defined using classical orbital elements: inclination = 97°, RAAN = 0°, semi-major axis of approximately 6878 km, corresponding to an orbital altitude of 500 km, argument of perigee = 0°, and initial mean anomaly = 5.01143×10^{-17}. For simplicity, the orbit was assumed to be circular with an eccentricity equal to zero, neglecting the effects of atmospheric drag and perturbations. In STK, this region was defined as a rectangular area target with latitude and longitude bounds that were approximately between 16.8°N–17.8° N and 44° E–47.1° E. The ROI was modeled as a rectangular target area in STK for consistency in the grid-based coverage evaluation. This simplification may include non-border terrain; therefore, the reported metrics represent coverage within the defined ROI window rather than a strictly border-aligned strip. A narrower corridor aligned with the border can modify the absolute coverage values and is identified as a potential refinement.

Reproducibility summary: All simulations were performed using STK v12.9 with a two-body propagator over a one-year scenario duration. The epoch, coordinate frame, orbital parameters, and sensor configuration were defined as described previously. The coverage analysis employed a grid-based area target with a specified mesh resolution and default STK access constraints under nadir-pointing assumptions.

For the simulation, two scenarios were assumed: the sun-synchronous orbit (SSO) scenario and a customized optimal orbital parameter scenario, where the inclination and RAAN values were changed to achieve satisfactory coverage quality and revisit time.

2.3.2. First scenario: baseline sun-synchronous orbit . The baseline SSO scenario utilized the orbital parameters

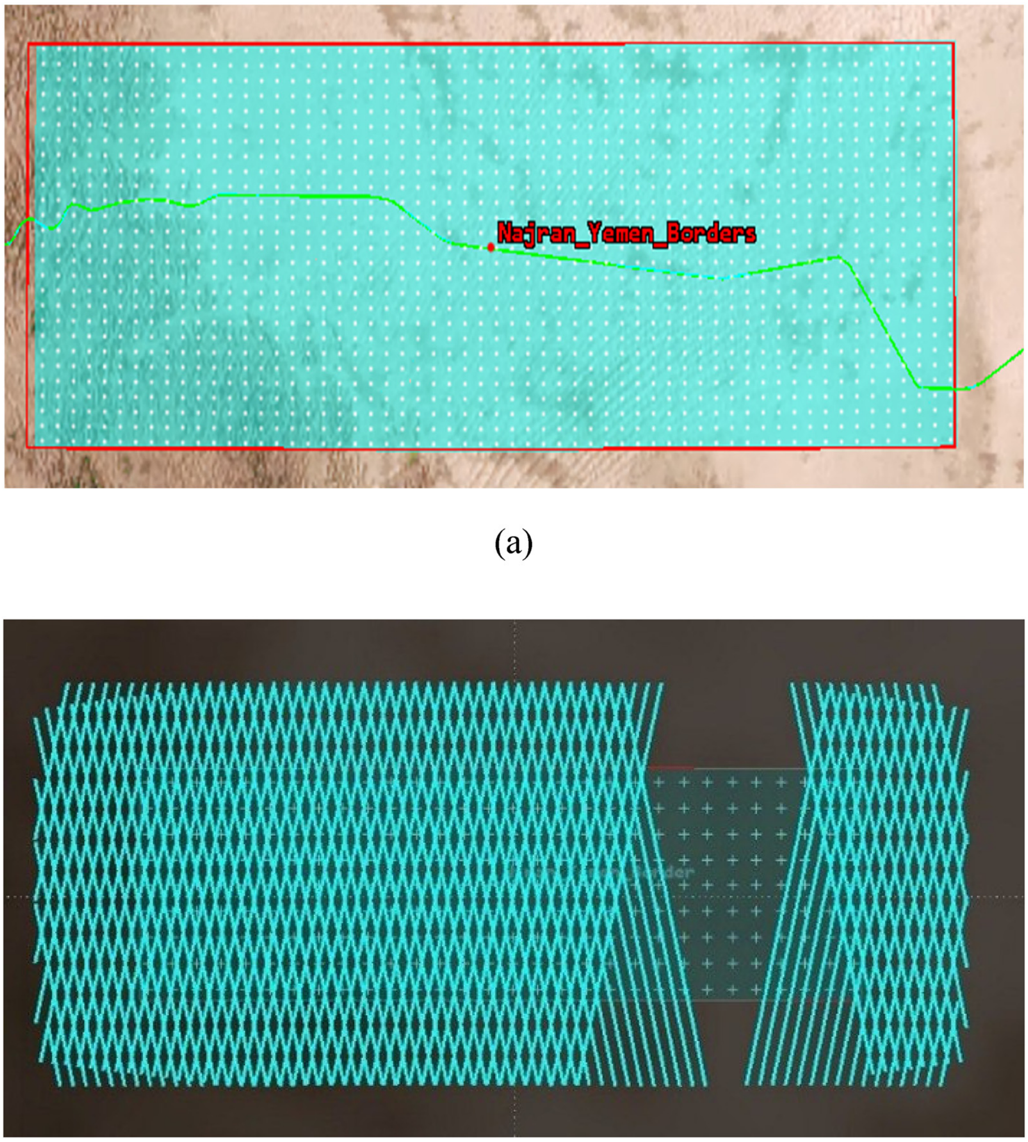

(a)

(b)

Figure 3. Satellite coverage footprint over the Najran–Yemen border: (a) 2D coverage projection, illustrating the sensor swath over the target region; (b) 3D representation of the CubeSat's nadir-viewing footprint projected onto the Earth's surface

described in Section 2.1, where the CubeSat was in the SSO at an altitude of 500 km. The sensor was modeled as a rectangular sensor with vertical and horizontal half-angles of 5° and 4°, respectively. The coverage definition object was used to conduct coverage analysis, in which the mesh was set to 0.1° to enable accurate coverage assessment. The coverage definition, together with the STK FoM module, was used to calculate the access periods between the CubeSat and the border area, defined as time intervals during which the satellite maintains a direct line of sight visibility of the target area. From these data, the key performance metrics were derived to evaluate the effectiveness of each scenario. These included the access duration, number of accesses, maximum revisit time, and coverage percentage. The analysis was repeated for multiple orbital configurations by varying inclination and RAAN, enabling direct comparison of how different orbital designs affect the frequency and duration of satellite passes over the targeted area. The optimal configuration was subsequently selected based on these comparative results, as discussed in Section 3.

2.3.3. Second scenario: customized optimal orbital parameters. In this scenario, the orbital inclination and RAAN were changed across a range appropriate for the latitude and longitude of the ROI. This test was conducted to determine the values that provided the best coverage performance. The satellite orbit was propagated using the STK J2 perturbation propagator, which accounts for the Earth's oblateness effects and the associated nodal regression. The atmospheric drag and higher-order perturbations were neglected. The second scenario provides a meaningful comparison to evaluate how different orbital parameters affect the number of accesses, coverage percentage, and revisit time.

3. RESULTS AND DISCUSSION

3.1. Coverage Metrics (Figure of Merit Results). Figure 3 shows the satellite footprint coverage of the ROI as 2D and 3D maps that align with the results of the four main performance parameters listed in Table 2. The parameters describe how well the satellite observed the Najran–Yemen border during the one-year simulation period. The first is the number of accesses, which represents how many times the satellite observed the target

Table 4. *Effect of RAAN on coverage performance (inclination fixed at 20°)*

RAAN	Number of accesses	Access duration (s)	Average revisit time (days)	Average coverage percentage (%)
30°	340	6.250	4.363	0.1642
60°	341	6.261	4.318	0.1662
90°	344	6.267	9.087	0.1679
120°	434	6.261	4.322	0.1660
180°	338	6.235	9.627	0.1636

area. The second parameter is the average access duration, which indicates how long the satellite could continuously see the region during each successful pass. The third parameter is the revisit time, which indicates the time gap between passes over the target area, and fourth, the average percentage of coverage, indicates the part of the target area that could be seen successfully. The results for the four parameters demonstrate that the baseline SSO provided weak, infrequent coverage and could not support continuous monitoring of the target region. This finding is attributed to the fact that the SSO has an inclination range from 97° to 98°, which leads to a low access number (127 passes per year) in the low-ground track of the altitude of the ROI. Although the access duration and average revisit time were marginally acceptable, the coverage percentage was quite low because the orbit was nearly polar, providing SSO coverage of a limited portion of the ROI.

3.2. Second Scenario: Customized Optimal Orbital Parameters.

3.2.1. Inclination study – results and interpretation. Table 3 shows the effect of varying the orbital inclination on the coverage performance of the CubeSat over the Najran–Yemen border region. All reported statistics represent the mean values averaged over all grid points within the ROI generated using the STK Coverage Definition and FoM tools. Revisit time values were exported from STK in seconds and converted to days by dividing by 86,400. The coverage percentage corresponds to the STK Percent Time Covered (Percent Satisfied) metric.

The results show the relationship between the inclination angle and access opportunities. For lower angles, such as those

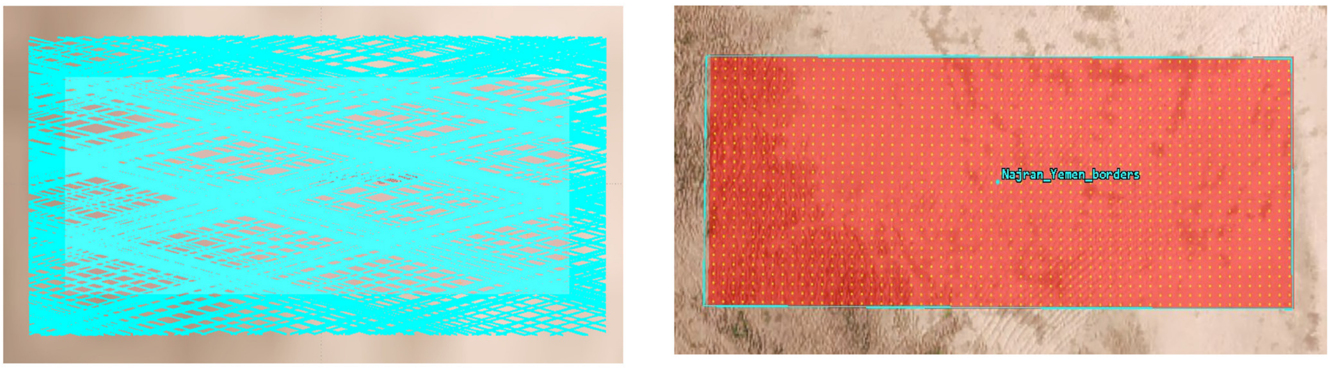

(a) (b)

Figure 4. Satellite coverage footprint over the Najran–Yemen Border: (a) 2D coverage projection, illustrating the sensor swath over the target region; (b) 3D representation of the CubeSat's nadir-viewing footprint projected onto the Earth's surface

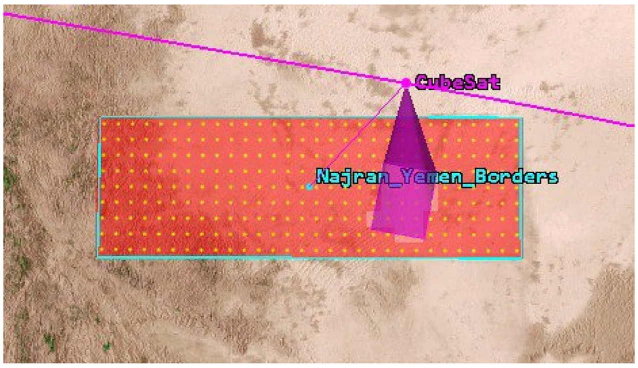

Figure 5. Sensor boresight alignment with the Najran–Yemen border during an access event

between 20° and 30°, the 20° angle provided better visibility. It had the highest number of access points at 335, with a short revisit time per grid point of 9.355 days. The 25° angle provided a slightly lower number of accesses, but achieved the longest access duration and the highest average coverage percentage at 0.2603%. This result suggests more continuous observation during each pass. As the angles increased beyond 30°, there was a significant decrease in both the number of accesses and coverage percentage. This result shows that these orbits do not work well in the latitude of the target area (17° N). Therefore, the best angles for monitoring the Najran–Yemen border region are 20° and 25°. The 25° angle is better for coverage duration and continuity, whereas a 20° angle is preferred for access frequency.

3.2.2. RAAN study – results and interpretation. Table 4 shows the effect of RAAN variation (30°–180°) while keeping the inclination fixed at 20° . The results show that the RAAN influences the coverage quality. RAAN values of 30°, 60°, and 120° exhibited comparable performance, whereas RAAN = 90° showed significantly higher revisit time and degraded temporal performance, with access between 334 and 344 and coverage percentages ranging from 0.1642% to 0.1660%. This behavior can be explained by the role of the RAAN in defining the longitudinal alignment of the orbital plane relative to Earth's rotation. Changing the RAAN effectively shifts the ground track pattern longitudinally, thereby modifying the temporal alignment between the satellite passes and the ROI. For certain RAAN values, the orbital plane intersects the target region more favorably, leading to shorter temporal gaps and improved revisit characteristics, as reported in orbital coverage design studies [14]. The highest accessibility (434) was achieved at RAAN = 120°, which also provided a considerable coverage percentage (0.1660%) versus radius and a relatively short average revisit time (4.322 days), the lowest in extent, resulting in the orbital plane with this value of RAAN optimally timing the satellite crossover with respect to the target area. On average, the best RAAN range was approximately 60° to 120°, and RAAN = 120° provided the maximum performance for various simulated values.

3.2.3. Sensor footprint and coverage visualization. To validate the results for the best orbital parameters, a satellite with the same values was simulated. The best-performing configuration identified in this sensitivity analysis was 20° inclination and RAAN = 120°, which provided a clear visual confirmation of the numerical results. Figure 4(a) shows the footprint coverage distribution, where the dense and repeated swaths across the Najran–Yemen border confirmed the frequent access opportunities reported in the inclination and RAAN tables. Figure 4(b) shows the coverage grid, in which the uniformly populated grid points demonstrate that the sensor repeatedly intersected

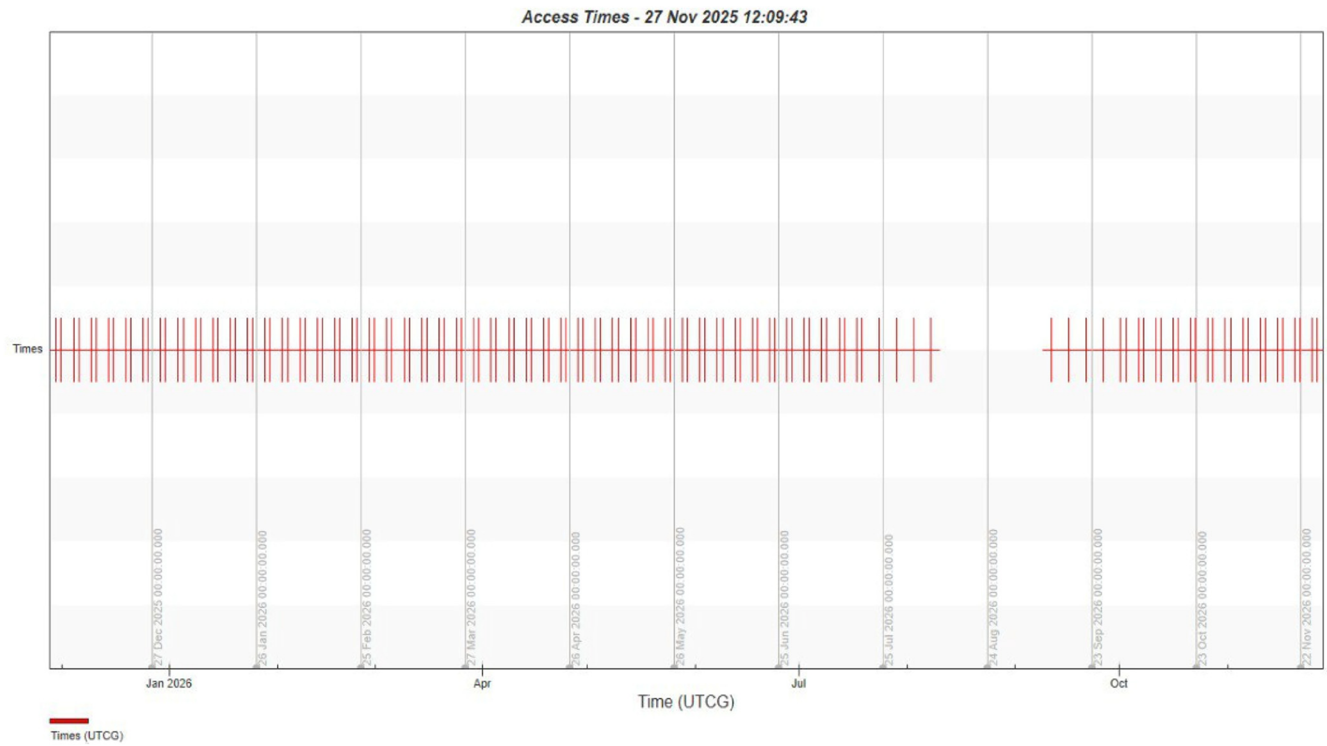

Figure 6. Access timeline for Scenario 1 (SSO)

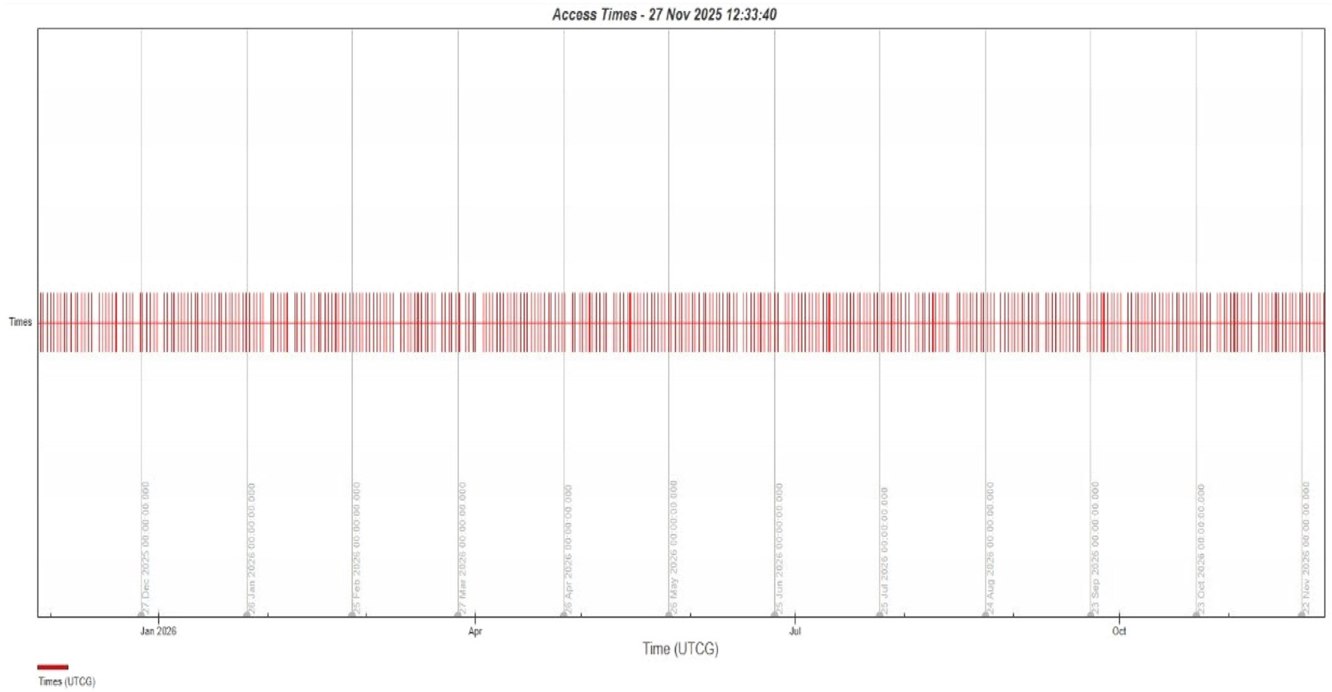

Figure 7. Access timeline for Scenario 2 (20° inclination, RAAN = 120°)

the entire region, supporting the improved coverage percentage observed in the results.

Finally, Figure 5 shows the sensor boresight directly aligned with the target area during an actual access event, confirming that each computed access corresponds to true line-of-sight visibility. Together, these three figures validate that the optimized orbit achieves strong geometric alignment with the region, thereby supporting the quantitative findings.

Figures 6 and 7 compare the temporal distribution of access events for Scenarios 1 and 2, respectively. Scenario 1 (SSO) exhibited long gaps between successive accesses, particularly visible during the mid-year, when access opportunities became sparse and irregular. This pattern reflects the misalignment between the Sun-synchronous repeat cycle and the elongated east-west orientation of the Najran–Yemen border region. In contrast, Scenario 2 (20° inclination, RAAN = 120°) demonstrated a much denser and more continuous access timeline, with events distributed consistently throughout the year. This behavior confirms that aligning the orbital plane with the region's latitude significantly increases the revisit frequency and reduces long coverage gaps. Therefore, Scenario 2 provides substantially superior temporal coverage and more operationally reliable monitoring performance than the baseline SSO configuration.

4. MODELING ASSUMPTIONS AND PRACTICAL CONSIDERATIONS

The results of this study should be interpreted within the scope of the adopted modeling assumptions. The simulated CubeSat was equipped with a nadir-pointing optical sensor that provided an approximate GSD of 25 m at 500-km altitude. At this spatial resolution, the system is more suitable for wide-area contextual monitoring than for the direct identification of small objects such as individual vehicles or persons. Therefore, the results primarily reflect improvements in temporal access and regional observation opportunities rather than high-resolution tactical surveillance capability.

The reported coverage percentages and revisit metrics were calculated using geometric line-of-sight analysis with STK Coverage and FoM tools. The simulations assumed ideal imaging conditions and did not incorporate atmospheric attenuation, cloud cover, sensor noise, or operational task constraints. In addition, the analysis focused on geometric access without explicitly enforcing daylight or illumination constraints. Consequently, the comparison between the SSO and non-SSO configurations represents relative geometric performance rather than illumination-optimized imaging feasibility.

5. CONCLUSIONS

In this study, the effect of orbital parameters on CubeSat performance was investigated in monitoring the border region of Najran in Saudi Arabia and Yemen. The results show that the SSO, which was used as the basic model, has limited temporal coverage and long gaps between revisits. In contrast, the second scenario demonstrates that an inclination from 20° to 25° and RAAN of approximately 120° significantly increase the number of accesses and reduce revisit time. Overall, the optimized orbit represents a significant improvement in coverage performance. This finding demonstrates the potential of a single CubeSat to improve temporal access opportunities for regional border observations. These results show that orbital parameter optimization could be an effective and feasible approach to enhance regional monitoring capabilities without increasing system complexity or using multiple satellites. However, these findings are based on an idealized geometric analysis and should be interpreted within the scope of the modeling assumptions. It is worth noting that the simulations in the current study assumed geometric coverage conditions with a constant altitude and nadir-pointing arrangement and did not consider atmospheric conditions, daylight constraints, or adaptive pointing models.

These limitations indicate that the reported improvements reflect geometric access potential rather than operational performance. Future studies could include the assessment of off-nadir imaging, the incorporation of daylight constraints, and the consideration of propulsion-enabled orbit maintenance and agile pointing strategies, which have become increasingly feasible in modern nanosatellite platforms[15]. Such extensions would provide a more comprehensive evaluation of CubeSat performance under realistic mission conditions and support the practical implementation of optimized orbital configurations.

AFFILIATIONS AND AUTHOR DETAILS

Undergraduate Author

Ghadi Mahdi Al Amer – *Department of Aerospace Engineering, King Fahd University of Petroleum & Minerals, Dhahran 31261, Saudi Arabia;* 0009-0007-7377-9704
Email: s202280560@kfupm.edu.sa

Corresponding Author

Asia Saeed Kajo Habila – *Research Mentor, Postdoctoral Fellow, Interdisciplinary Research Center for Aviation and Space Exploration, King Fahd University of Petroleum & Minerals, Dhahran 31261, Saudi Arabia;* 0000-0002-6155-2832
Email: asia.habila@kfupm.edu.sa

ACKNOWLEDGEMENTS

The author acknowledges the support of the Interdisciplinary Research Center for Aviation and Space Exploration at King Fahd University of Petroleum and Minerals (KFUPM). The author also thanks the research advisor for her guidance throughout the Independent Research course and her helpful feedback on this work.

REFERENCES

(1) Haloho, L. S. & Supriyadi, A. A. Utilization of satellite technology in communication systems, disaster monitoring, border surveillance, and military intelligence: A literature review. Remote Sens. Technol. Def. Environ. 1, 36–44 (2024).

(2) Tummala, A. R. & Dutta, A. An overview of Cube-satellite propulsion technologies and trends. Aerospace 4, 58 (2017).

(3) Aval, R. E. & Khazaee, M. Health monitoring system of CubeSats: A comprehensive review (2023).

(4) Eshaq, M. et al. CubeSat flight software: Insights and a case study. J. Spacecr. Rockets 1–18 (2025).

(5) Rainjonneau, S. et al. Quantum algorithms applied to satellite mission planning for Earth observation. IEEE J. Sel. Top. Appl. Earth Obs. Remote Sens. 16, 7062–7075 (2023).

(6) Al Jazeera. Saudi-led coalition says it destroyed missile targeting Najran (2020).

(7) Selva, D. & Krejci, D. A survey and assessment of the capabilities of CubeSats for Earth observation. Acta Astronaut. 74, 50–68 (2012).

(8) Santilli, G. et al. CubeSat constellations for disaster management in remote areas. Acta Astronaut. 145, 11–17 (2018).

(9) Wikipedia contributors. Orbital elements. Wikipedia (2025).

(10) ANSYS. What is a CMOS image sensor? (2025).

(11) Simulation analysis of coverage performance of LEO satellite communication system based on STK. Proc. SPIE (2026).

(12) Bhushan, S. et al. Automated digital elevation model generation from very-high-resolution Planet SkySat triplet stereo and video imagery. ISPRS J. Photogramm. Remote Sens. 173, 151–165 (2021).

(13) Funada, K., Black, J. & Lowe, T. Analysis of a CubeSat orbit using STK (2023).

(14) Ahmed, A. A. A comprehensive review of satellite orbital placement and coverage optimization for low Earth orbit satellite networks: Challenges and solutions. Network 5, 32 (2025).

(15) Fevgas, G. et al. Advances in remote sensing and propulsion systems for Earth observation nanosatellites. Future Internet 17 (2025).